

## Cation Control of Pore and Channel Size in Cage-Based Metal–Organic Porous Materials

Roger G. Harrison,\*<sup>†</sup> O. Danny Fox,<sup>†</sup> Mark O. Meng,<sup>†</sup> N. Kent Dalley,<sup>†</sup> and Leonard J. Barbour<sup>‡</sup>

Department of Chemistry and Biochemistry, Brigham Young University, Provo, Utah 84601, and Department of Chemistry, University of Missouri–Columbia, Columbia, Missouri 65211

Received November 2, 2001

Porous materials resembling zeolites that are composed of organic and inorganic building units were synthesized and characterized. Control of pore and channel size was achieved by using different-sized cations. The metal-assembled, anionic cage molecule,  $\text{Co}_4\text{1}_2^{8-}$ , with a hydrophobic cavity and four carboxylate rich arms, was used as a structural unit for the formation of materials with pores and channels. When assembled into a solid material with dications ( $\text{Mg}^{2+}$ ,  $\text{Ca}^{2+}$ ,  $\text{Sr}^{2+}$ , and  $\text{Ba}^{2+}$ ),  $\text{Co}_4\text{1}_2^{8-}$  arranges into sheets of cages linked together by cations. The series of materials based on  $\text{Co}_4\text{1}_2^{8-}$  and containing alkaline earth cations was characterized using X-ray crystallography. The magnesium material packs with cages close together, has small channels, and has cation–carboxylate linkages in three dimensions. The calcium material has cages packed with voids between them and has  $5 \times 10 \text{ \AA}$  channels and  $10 \times 21 \text{ \AA}$  pores. The strontium and barium materials also pack with voids between the cages and similarly to each other. They have  $11 \times 13 \text{ \AA}$  and  $11 \times 11 \text{ \AA}$  channels and  $10 \times 27 \text{ \AA}$  and  $9 \times 27 \text{ \AA}$  pores, respectively. Each of these materials has many (20–50) solvent water molecules associated with each cage. The associated water can be removed from and adsorbed by the materials. The heat of water binding has been measured to be  $-52 \text{ kJ/mol}$  ( $\text{Mg}_4\text{Co}_4\text{1}_2$ );  $-47 \text{ kJ/mol}$  ( $\text{Ca}_4\text{Co}_4\text{1}_2$ );  $-48 \text{ kJ/mol}$  ( $\text{Sr}_4\text{Co}_4\text{1}_2$ );  $-49 \text{ kJ/mol}$  ( $\text{Ba}_4\text{Co}_4\text{1}_2$ ).

### Introduction

Porous silica- and alumina-based materials are of great past and current interest because of their use in catalysis and separations. A relatively new class of porous materials which contain organic and inorganic components is likely to have similar properties. These metal–organic materials have pores and channels similar to zeolites; however, they are assembled with organic compounds and often have organic substituents lining the pores and channels. They thus have unique properties and are being investigated for chemical separation properties, catalytic activity, and the ability to store small molecules.<sup>1</sup> One very important aspect of this new field is the development of ways to control the size and shape of the pores and channels and the polarity of the surrounding groups.<sup>2</sup> Both the organic substituents and the metal ions

can be used to change the size, shape, and polarity of the pores and channels.

Various ligands with organic spacers between coordinating atoms when bound to metal ions can be used to produce porous materials. Simple bidentate ligands can be used; however, most simple ligands that invoke little directional bonding often promote the formation of metal-assembled polymers.<sup>3</sup> Metal coordination polymers are of interest but in most cases are not porous. It is beneficial when the ligand invokes some degree of bonding directionality, which forces the metal ions to coordinate at certain angles and in certain places. Nitrogen-containing ligands, such as pyridine and nitrile, have been used successfully to form porous materials.<sup>2a,4</sup> In addition to nitrogen-containing ligands are oxygen-containing ligands, principally those with carboxylate groups.<sup>5</sup> The development of new porous materials and materials with specific properties will come in part through the use of more

\* To whom correspondence should be addressed. Phone: 801-378-8096. Fax: 801-378-5474. E-mail: roger\_harrison@byu.edu.

<sup>†</sup> Brigham Young University.

<sup>‡</sup> University of Missouri–Columbia.

(1) (a) Hagrman, P. J.; Hagrman, D.; Zubietta, J. *Angew. Chem., Int. Ed.* **1999**, *38*, 2638. (b) Blake, A. J.; Champness, N. R.; Hubberstey, H.; Li, W.-S.; Withersby, M. A.; Schröder, M. *Coord. Chem. Rev.* **1999**, *183*, 117. (c) Yaghi, O. M.; Li, H.; Cavis, C.; Richardson, D.; Groy, T. L. *Acc. Chem. Res.* **1998**, *31*, 474.

(2) (a) Eddaoudi, M.; Molar, D. B.; Li, H.; Chen, B.; Reineke, T. M.; O'Keeffe, M.; Yaghi, O. M. *Acc. Chem. Res.* **2001**, *34*, 319. (b) Kiang, Y.-H.; Gardner, G. B.; Lee, S.; Xu, Z.; Lobkovsky, E. B. *J. Am. Chem. Soc.* **1999**, *121*, 8204.

(3) (a) Zaworotko, M. J. *Angew. Chem., Int. Ed.* **2000**, *39*, 3052. (b) Batten, S. R.; Robson, R. *Angew. Chem., Int. Ed.* **1998**, *37*, 1461. (c) Fujita, M. *Acc. Chem. Res.* **1999**, *32*, 53.

elaborate ligands.<sup>6</sup> The use of more elaborate organic-based building units is just beginning to be explored.

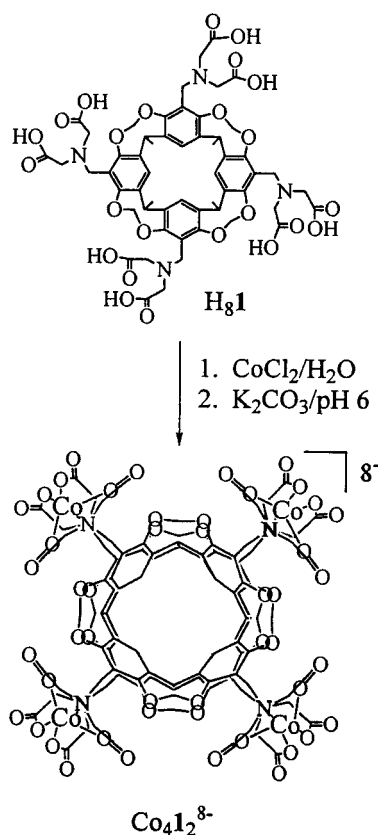
The metal ion also plays a critical role in the assembly of the porous material. Its coordination number, ligand preference, and preferred coordination geometry are all important to what type of material forms. A wide range of metal ions has been used including group I ions, lanthanides, and transition metals.<sup>4–6</sup> For these metals to be used successfully, they must be matched with the correct ligand.

During our research on metal-assembled cage complexes,<sup>7</sup> we have found that, in the presence of the right cation, cages pack into materials that are porous.<sup>8</sup> Once we discovered that the cages can act as building blocks to make materials with pores and channels, we sought to change pore and channel size and shape. Herein, we report on how pore and channel size and shape can be changed by using different group II cations to assemble the cages. The group II cations  $\text{Mg}^{2+}$ ,  $\text{Ca}^{2+}$ ,  $\text{Sr}^{2+}$ , and  $\text{Ba}^{2+}$ , with their different sizes and coordination number preferences, induce cages to pack in different ways. As a result, channels and pores of varying sizes are created. Because these materials have both organic and inorganic components, the resulting pores are surrounded by both polar and nonpolar groups. Water molecules, which can be removed by heating and adsorbed back again by cooling, occupy the pores. The heat of water adsorption for the four group II materials has been measured and falls within the range typical of that for zeolitic materials.

## Results and Discussion

The synthesis of the materials starts with the formation of cobalt-assembled cages. To form the cages,  $\text{CoCl}_2$  is added

Scheme 1



to an aqueous solution of protonated iminodicarboxylate resorcinarene **1** and the pH is raised to above 5 to promote cobalt coordination (Scheme 1). After the cages have been formed, a group II cation is added to make the desired  $\text{Mg}^{2+}$ ,  $\text{Ca}^{2+}$ ,  $\text{Sr}^{2+}$ , or  $\text{Ba}^{2+}$  materials. The materials are crystallized by layering 2-propanol over the aqueous solutions of the appropriate group II and cage mixtures. For the magnesium material, crystal growth takes weeks, while for the calcium, strontium, and barium materials, single crystals are deposited within days. The cage complex  $\text{Co}_412^{8-}$  has two resorcinarene molecules brought together by four  $\text{Co}^{2+}$  ions in such a manner that a pocket is formed between them. The cobalt centers are six coordinate and ligated by both resorcinarenes, via two amine nitrogens and four carboxylate oxygens. The centers are also dianionic and coplanar and lie at  $90^\circ$  with respect to each other (Scheme 1). The oxygen atoms from the carboxylate groups point away from the cages in four directions, providing coordination centers for group II metal cations.

**$\text{Mg}_2\text{K}_4\text{Co}_412$  Structure.** The Mg material is structurally very different from the Ca, Sr, and Ba materials. The  $\text{Co}_412^{8-}$  cages are brought together by magnesium ions in all three dimensions. In one plane, six cages come together with their carboxylate groups bonding to magnesiums and their methyl groups pointing at the methyl groups of other cages (Figure 1). This arrangement of cages leaves very little empty space between cages. The magnesium ions in the plane of the cages are hydrophobic centers, and many waters surround them. It is likely that potassiums are also located in this region; however, due to their disorder they cannot be resolved using

- (4) (a) Tabares, L. C.; Navarro, J. A. R.; Salas, J. M. *J. Am. Chem. Soc.* **2001**, *123*, 383. (b) Hong, M.; Zhao, Y.; Su, W.; Cao, R.; Fujita, M.; Zhou, Z.; Chan, A. S. C. *Angew. Chem., Int. Ed.* **2000**, *39*, 2468. (c) Noro, S.; Kitagawa, S.; Kondo, M.; Seki, K. *Angew. Chem., Int. Ed.* **2000**, *39*, 2082. (d) Carlucci, L.; Ciani, G.; Moret, M.; Proserpio, D. M.; Rizzato, S. *Angew. Chem., Int. Ed.* **2000**, *39*, 1506. (e) Keller, S. W.; Lopaz, S. *J. Am. Chem. Soc.* **1999**, *121*, 6306. (f) Gudbjartson, H.; Biradha, K.; Poirier, K. M.; Zaworotko, M. J. *J. Am. Chem. Soc.* **1999**, *121*, 2599. (g) Goodgame, D. M. L.; Grachvogel, D. A.; Williams, D. J. *Angew. Chem., Int. Ed.* **1999**, *38*, 153. (h) Kepert, C. J.; Rosseinsky, M. J. *Chem. Commun.* **1999**, 375. (i) Wang, Q.; Wu, X.; Zhang, W.; Sheng, T.; Lin, P.; Li, J. *Inorg. Chem.* **1999**, *38*, 2223. (j) Abrahams, B. F.; Jackson, P. A.; Robson, R. *Angew. Chem., Int. Ed.* **1998**, *37*, 2656. (k) Kondo, M.; Yoshitomi, T.; Seki, K.; Matsuzaka, H.; Kitagawa, S. *Angew. Chem., Int. Ed. Engl.* **1997**, *36*, 1725.
- (5) (a) Chen, B.; Eddaoudi, M.; Reineke, T. M.; Kampf, J. W.; O'Keeffe, M.; Yaghi, O. M. *J. Am. Chem. Soc.* **2000**, *122*, 11559. (b) Reineke, T. M.; Eddaoudi, M.; Moler, D.; O'Keeffe, M.; Yaghi, O. M. *J. Am. Chem. Soc.* **2000**, *122*, 4843. (c) Evans, O. R.; Lin, W. *Inorg. Chem.* **2000**, *39*, 2189. (d) Pan, L.; Woodlock, E. B.; Wang, X.; Zheng, C. *Inorg. Chem.* **2000**, *39*, 4174. (e) Zhu, J.; Bu, X.; Feng, P.; Stucky, G. D. *J. Am. Chem. Soc.* **2000**, *122*, 11563. (f) Reineke, T. M.; Eddaoudi, M.; Fehr, M.; Kelley, D.; Yaghi, O. M. *J. Am. Chem. Soc.* **1999**, *121*, 1651. (g) Li, H.; Eddaoudi, M.; O'Keeffe, M.; Yaghi, O. M. *Nature* **1999**, *402*, 276.
- (6) (a) Lee, E.; Kim, J.; Heo, J.; Whang, D.; Kim, K. *Angew. Chem., Int. Ed.* **2001**, *40*, 399. (b) Bennett, M. V.; Shores, M. P.; Beauvais, L. G.; Long, J. R. *J. Am. Chem. Soc.* **2000**, *122*, 6664. (c) Moon, M.; Kim, I.; Lah, M. S. *Inorg. Chem.* **2000**, *39*, 2710. (d) Heo, J.; Kim, S.-Y.; Whang, D.; Kim, K. *Angew. Chem., Int. Ed.* **1999**, *38*, 641. (e) Orr, G. W.; Barbour, L. J.; Atwood, J. L. *Science* **1999**, *285*, 1049.
- (7) (a) Fox, O. D.; Leung, J. F.; Hunter, J. M.; Dalley, N. K.; Harrison, R. G. *Inorg. Chem.* **2000**, *39*, 783. (b) Fox, O. D.; Dalley, N. K.; Harrison, R. G. *J. Am. Chem. Soc.*, **1998**, *120*, 7111.
- (8) Harrison, R. G.; Dalley, N. K.; Nazarenko, A. Y. *Chem. Commun.* **2000**, 1387.

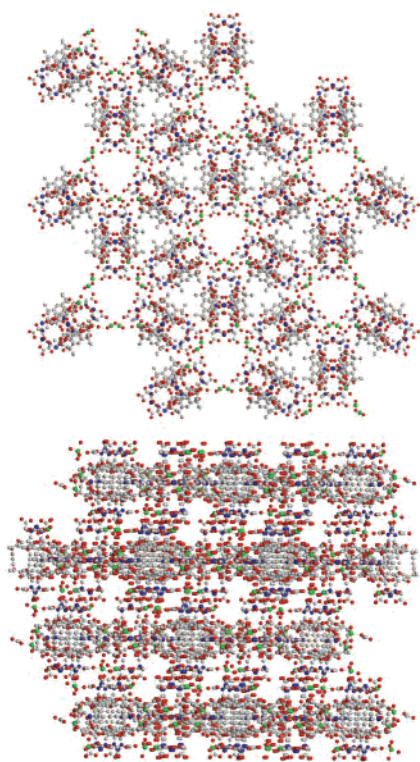


**Figure 1.** Structure of Mg-assembled material. (a, top) Cage packing in two dimensions. Each subunit is a cage with its carboxylate arms pointing in the plane of the paper and in and out of the paper. Six cages come together with their carboxylate arms bridged by magnesium ions. (b, bottom) Stacking of layers of cages showing the ABCA packing of the cages and the connection of cages between layers. (Hydrogens and interstitial waters have been removed for clarity. Color coding: gray = carbon, blue = nitrogen, red = oxygen, dark blue = cobalt, green = magnesium.)

X-ray crystallography. Potassium ions are incorporated into this material as seen by elemental analysis, but not into the other materials, even though all of the materials are synthesized in the presence of potassium. We do not understand yet why potassium is incorporated into this material.

The other two carboxylate groups of each cage point above and below the plane of cages. These two groups connect to magnesiums of another layer of cages. This results in layers of cages being offset from each other and forming an ABCA type cage packing arrangement (Figure 1). There is very little unoccupied space between the layers of cages, and thus, only small channels are generated. These channels are lined with carboxylate groups and magnesiums and are occupied with water molecules. The overall packing in the magnesium material is much more condensed than in the other three materials, which can be attributed to the magnesium ions' smaller size and preference for a lower coordination number.

**Ca<sub>4</sub>Co<sub>4</sub>I<sub>2</sub> Structure.** Each cage with its four carboxylate arms binds to four calciums, which bond to other cages. The calciums connect two cages together and in so doing create a two-dimensional array of cages (Figure 2). Voids are formed between neighboring cages, and water molecules bound to calciums surround them. The cages alternate above and below each other with their carboxylate arms at the side

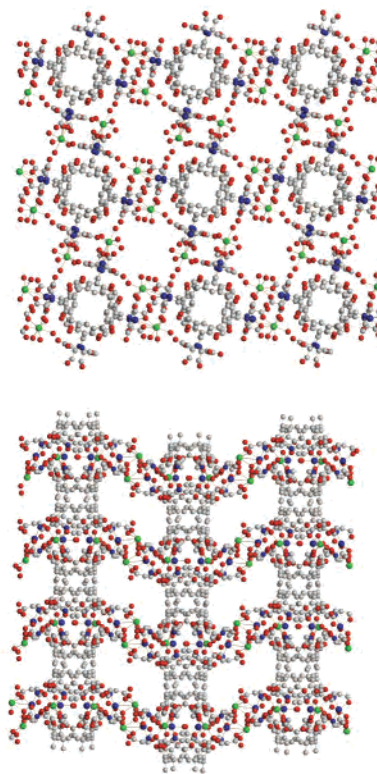


**Figure 2.** Structure of the Ca-assembled material. (a, top) A two-dimensional array of cages is formed by the calciums bridging the carboxylate arms of the cages. All of the carboxylate groups are in the same plane as the cages. Note the voids created between the cages. (b, bottom) The stacking of the layers of cages results in channels that run between the layers and pores that span the space between every other layer of cages. The second and fourth layers of cages are behind the first and third layers. (Hydrogens and interstitial waters have been removed for clarity. Color coding: gray = carbon, blue = nitrogen, red = oxygen, dark blue = cobalt, green = calcium.)

**Table 1.** Comparison of Packing Arrangement, Channel Size, and Pore Size for the Group II Materials

compound	packing <sup>a</sup>	channel size (Å) <sup>b</sup>	pore size (Å) <sup>b</sup>
Mg <sub>2</sub> K <sub>4</sub> Co <sub>4</sub> I <sub>2</sub>	ABCA	small	na
Ca <sub>4</sub> Co <sub>4</sub> I <sub>2</sub>	ABAB	5.4 × 10	10 × 20.9
Sr <sub>4</sub> Co <sub>4</sub> I <sub>2</sub>	ABCD	11 × 13	10 × 27.5
Ba <sub>4</sub> Co <sub>4</sub> I <sub>2</sub>	ABCD	11 × 11	9.2 × 27

<sup>a</sup> The packing arrangement of cages along the *c* axis. <sup>b</sup> Distance between the electron clouds of two group II cations which lie across the void. The 6-coordinate radius for Mg<sup>2+</sup> and 8-coordinate radii for Ca<sup>2+</sup>, Sr<sup>2+</sup>, and Ba<sup>2+</sup> were used.

and slightly above and below each other. The next layer of cages could position cages to fill the voids created in the first layer; however, they do not. Instead, the cages are positioned above the carboxylate groups and calcium ions. The third layer lies directly over the first layer creating an ABAB cage packing arrangement. This type of cage packing results in pores that have 13 Å widths and 21 Å lengths (Table 1). The widths span between two cages, and the length runs from the calciums of every other layer of cages. The channels that connect the pores lie between the layers and run parallel to each other in one direction only. In the other direction, the cages form a wall without channels. Methyl and carboxylate groups line the channels, and water mol-



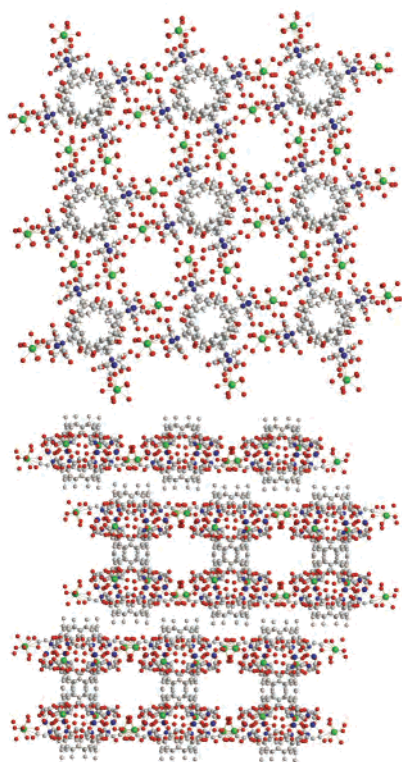


**Figure 3.** Structure of the Sr-assembled material. (a, top)  $\text{Sr}^{2+}$  ions bond between carboxylate arms of the cages and bring the cages together into a two-dimensional array. Voids are created between the cages. The layers of cages pack together, creating channels that run perpendicular to each other and between the layers. Pores linked together by the channels span the space between alternating layers of cages. The third and fourth layers of cages lie behind the first, second, and fifth layers. (Hydrogens and interstitial waters have been removed for clarity. Color coding: gray = carbon, blue = nitrogen, red = oxygen, dark blue = cobalt, green = strontium.).

ecules reside within them. Their width ( $10 \text{ \AA}$ ) is almost double their height ( $5.4 \text{ \AA}$ ).

**$\text{Sr}_4\text{Co}_4\text{I}_2$  Structure.** As with the calcium material, the cations, in this case  $\text{Sr}^{2+}$ , bridge between carboxylate groups from two cages and result in the formation of an array of cages (Figure 3). Again, as with the calcium material, the cages of the next layer do not occupy the voids, but position themselves over the cation bridges. However, unlike the calcium material, the cages lie in the same plane and the strontium ions bridge each other side by side. Furthermore, the third layer packs in a new position, as does the fourth layer, which creates an ABCD cage packing arrangement. The cage packing promoted by strontium results in strontiums all lying in the same plane and results in pores that have greater length ( $28 \text{ \AA}$ ) than those in the calcium material. The pore widths of  $10 \text{ \AA}$ , however, are very similar to those of the calcium material. The channels that connect the pores run perpendicular to each other and between different layers of cages. They are significantly larger,  $11 \times 13 \text{ \AA}^2$ , than the channels in the calcium material, and, unlike the channels in the calcium material, they run in two directions. The channels run between every layer of cages but do so in alternating directions. The channels are lined by methyl and carboxylate groups and are occupied by water molecules.

**$\text{Ba}_4\text{Co}_4\text{I}_2$  Structure.** Similar to the other group II cations in the magnesium, calcium, and strontium materials, barium cations bind to carboxylates of two cages and link the cages together. As is also observed in the calcium and strontium materials, voids are created between the cages when they are assembled by barium cations. The bariums and cages lie in the same plane, and the layers of cages pack in an ABCD arrangement, as they do in the strontium material (Figure 3). The pores in the material are  $9 \text{ \AA}$  wide by  $27 \text{ \AA}$  long and are similar in size to the strontium material's pores. The channels are likewise similar to the strontium material's and are  $11 \times 11 \text{ \AA}$ . However, the pores and channels are slightly smaller than they are in  $\text{Sr}_4\text{Co}_4\text{I}_2$ , due in part to the increased radii of barium cations compared to strontium cations. As in the strontium material, the channels run perpendicular to each other between the layers of cages. The channels and pores are lined with methyl and carboxylate groups.

**Water Adsorption.** As is seen in the crystal structures of each of these materials, they contain many water molecules, from 20 to 50 per each  $\text{M}_4\text{Co}_4\text{I}_2$  molecule. These waters can be removed and reabsorbed by the materials. Simply blowing air over the materials removes some of the waters, while heating removes the remainder. When a small sample of material, 1–3 mg, is placed on a thermogravimetric balance, and the material is heated while nitrogen is blowing over it, the material steadily loses water until  $120 \text{ }^\circ\text{C}$ . Cooling the material and blowing water vapor over it results in the material gaining weight and water being adsorbed. This process of desorption and adsorption can be repeated without a change in the amount of water adsorbed. The external appearance of the crystals does not change due to water loss. However, evidence for internal structural integrity was not obtained. The crystals do not give clear X-ray powder diffraction patterns before or after sorption, and single crystals exposed to air do not diffract well.

The materials lose about 15% of their weight when heated from  $25$  to  $180 \text{ }^\circ\text{C}$ . The number of water molecules lost per  $\text{M}_4\text{Co}_4\text{I}_2$  molecule is as follows: 26,  $\text{Mg}_2\text{K}_4\text{Co}_4\text{I}_2$ ; 20,  $\text{Ca}_4\text{Co}_4\text{I}_2$ ; 34,  $\text{Sr}_4\text{Co}_4\text{I}_2$ ; 31,  $\text{Ba}_4\text{Co}_4\text{I}_2$ . This accounts for an average of 6.5, 5, 8.5, and 8 water molecules per group II cation for the series from Mg, Ca, Sr, and Ba materials, respectively. The number of water molecules per cation increases, except for  $\text{Ca}_4\text{Co}_4\text{I}_2$ , as the cation size becomes larger, matching to some degree the ability of the cation to coordinate to more water molecules. The number of waters per  $\text{M}_4\text{Co}_4\text{I}_2$  unit determined thermogravimetrically is, in most cases, less than the number observed in the crystal structures because the TGA measurements were conducted with crystals exposed to air at  $25 \text{ }^\circ\text{C}$ , whereas the crystals used for X-ray analysis were analyzed in the presence of solvent water.

**Heat of Adsorption.** After observing the materials' ability to adsorb water, we attempted to measure the heat of adsorption of the water so as to measure the strength of water bonding, facilitating comparison of these materials to zeolites. The heat of adsorption is found by measuring the amount of water adsorbed at different temperatures and calculating equilibrium constants.<sup>9</sup> Plotting  $\ln K$  versus inverse temper-

ature yields a slope proportional to the heat of adsorption ( $\Delta H_{\text{ad}}$ ). We found the heats of adsorption to be as follows:  $-52$  kJ/mol,  $\text{Mg}_2\text{K}_4\text{Co}_4\text{I}_2$ ;  $-47$  kJ/mol,  $\text{Ca}_4\text{Co}_4\text{I}_2$ ;  $-48$  kJ/mol,  $\text{Sr}_4\text{Co}_4\text{I}_2$ ;  $-49$  kJ/mol,  $\text{Ba}_4\text{Co}_4\text{I}_2$ . This is over the temperature range  $25$ – $73$  °C with a water vapor pressure of  $20$  mmHg. At these low temperatures, the materials are in a state that is close to full water occupancy. The magnesium material's heat of adsorption is slightly greater than the others. However, all of the heats of adsorption are very similar, which indicates that water is being removed from similar sites within each material. The heats of adsorption are also indicative of strong attractive forces between the water molecules and the materials and can be attributed to the water molecules being hydrogen-bonded to each other and bound to the metal ions within the materials. These heats of water adsorption suggest that the strength of water binding in these materials is on the same order as that of the silica zeolites.<sup>10</sup> This is noteworthy, given the large organic component of these materials. Especially in the case of  $\text{Ca}_4\text{Co}_4\text{I}_2$ , there is a slight decrease in heats of adsorption as temperature increases ( $2$ – $6$  kJ/mol), which may imply that the sites of adsorption are changing with temperature.

## Conclusion

The cobalt-assembled cage compound  $\text{Co}_4\text{I}_2^{8-}$  can be used as a building unit to make porous materials. The four carboxylate-containing arms of  $\text{Co}_4\text{I}_2^{8-}$  bind to metal ions and act as linking units to assemble the cages into arrays. The packing of the arrays by group II cations creates materials with channels and pores. The size and dimensions of the pores and channels can be controlled by the group II cation used for assembly. Magnesium creates a tightly packed material, which has magnesiums linking the cages together in three dimensions. It has only small channels filled with water and no pores. Calcium, however, causes the formation of channels that run between layers of cages and that lead to pores. Materials with larger channels and pores can be formed by using strontium or barium in place of calcium. Also, strontium and barium cause the channels to run in two directions, unlike the calcium material, which has channels in only one direction of the material. Like calcium and unlike magnesium, strontium and barium create materials that have carboxylate–metal bonds in only one plane.

Removal of the water that resides within the pores can be achieved by heating the materials. Thirteen to seventeen percent of the materials' weight is water. The heats of water adsorption are similar for all of the materials ( $-46$  to  $-52$  kJ/mol) and similar to those of silica-containing zeolites.

## Experimental Section

**General.** All commercial reagents and solvents were used as supplied unless noted.  $\text{Ba}_4\text{I}_7$ ,  $\text{Ca}_4\text{Co}_4\text{I}_2$ ,<sup>8</sup> and  $\text{Ba}_4\text{Co}_4\text{I}_2$ <sup>7</sup> were

- (9) Do, D. D. *Adsorption Analysis: Equilibria and Kinetics*; Imperial College Press: London, 1998. (b) Drago, R. S.; Webster, C. E.; McGilvray, J. M. *J. Am. Chem. Soc.* **1998**, *120*, 538.  
 (10) A direct comparison of heats of adsorption is difficult because the literature values are often reported at intermediate adsorbent occupancies and ours is measured at high adsorbent occupancy. (a) Breck, D. W. *Zeolite Molecular Sieves*; Wiley: New York, 1974. (b) Szostak, R. *Molecular Sieves Principles of Synthesis and Identification*, 2nd ed.; Thomas Science: New York, 1998.

**Table 2.** Crystal Data and Structure Refinement for  $\text{Mg}_2\text{K}_4\text{Co}_4\text{I}_2$  and  $\text{Sr}_4\text{Co}_4\text{I}_2$

	$\text{Mg}_2\text{K}_4\text{Co}_4\text{I}_2$	$\text{Sr}_4\text{Co}_4\text{I}_2$
empirical formula	$\text{C}_{112}\text{H}_{104}\text{N}_8\text{O}_{48}\text{Co}_4\text{K}_4\text{Mg}_2 \cdot 20\text{H}_2\text{O}$	$\text{C}_{112}\text{H}_{104}\text{N}_8\text{O}_{48}\text{Co}_4\text{Sr}_4\text{Sr}_{3.2} \cdot 42.5\text{H}_2\text{O}$
fw (g mol <sup>-1</sup> )	3128.73	3656.26
<i>T</i> (K)	173(2)	293(2)
cryst syst	rhombohedral	tetragonal
space group	<i>R</i> 3 <i>c</i>	<i>I</i> 4 <sub>1</sub> / <i>a</i>
color of cryst	pink	pink
<i>a</i> (Å)	31.683(2)	19.911(2)
<i>b</i> (Å)	31.683(2)	19.911(2)
<i>c</i> (Å)	105.352(11)	54.257(9)
$\alpha$ (deg)	90	90
$\beta$ (deg)	90	90
$\gamma$ (deg)	120	90
<i>Z</i>	18	4
GOF	1.897	1.063
<i>R</i>	0.1365	0.0878
wR2	0.3465	0.3075

synthesized as previously published. TGA was run on a Seiko DSC/TGA workstation SSC5200H. MHW laboratories performed elemental analyses. ICP was done with a Perkin-Elmer optical emission spectrometer Optima 2000 DV.

**Synthesis of  $\text{Mg}_2\text{K}_4\text{Co}_4\text{I}_2 \cdot x\text{H}_2\text{O}$ .** The synthesis of  $\text{Mg}_2\text{K}_4\text{Co}_4\text{I}_2$  was done in a manner similar to the synthesis of  $\text{Ca}_4\text{Co}_4\text{I}_2 \cdot x\text{H}_2\text{O}$ . To  $\text{Ba}_4\text{I}$  (65.8 mg, 0.027 mmol) stirred in 4 mL of water and 1 mL of 1 M HCl was added  $\text{K}_2\text{SO}_4$  (34.0 mg, 0.195 mmol), and the resultant precipitate was removed by decantation. To the remaining solution were added  $\text{MgCl}_2$  (66.4 mg, 0.327 mmol) and  $\text{CoCl}_2 \cdot 6\text{H}_2\text{O}$  (19.6 mg, 0.082 mmol). The solution was brought to pH 6.1 with powdered  $\text{K}_2\text{CO}_3$ . The white precipitate that formed was removed, and the pink solution was layered with 2-propanol. Upon standing for 3 weeks at ambient temperature, pink crystals of  $\text{Mg}_2\text{K}_4\text{Co}_4\text{I}_2 \cdot x\text{H}_2\text{O}$  formed (30.6 mg, 0.0086 mmol, 64% yield). ICP analysis gave a 2:1:2 ratio of Co:Mg:K. Anal. Calcd for  $\text{C}_{112}\text{H}_{104}\text{Co}_4\text{Mg}_2\text{K}_4\text{N}_8\text{O}_{48} \cdot 50\text{H}_2\text{O}$ : C, 36.63; H, 5.56; N, 3.05. Found C, 36.29; H, 4.08; N, 3.16.

**Synthesis of  $\text{Sr}_4\text{Co}_4\text{I}_2 \cdot x\text{H}_2\text{O}$ .** Compound  $\text{Ba}_4\text{I}$  (100 mg, 0.0410 mmol) was stirred in 1 M hydrochloric acid (10 mL) until a clear solution was obtained. Water (10 mL) and  $\text{K}_2\text{SO}_4$  (80 mg, 0.46 mmol) were added, and the white precipitate of barium sulfate that formed was removed by filtration.  $\text{CoCl}_2 \cdot 6\text{H}_2\text{O}$  (40 mg, 0.168 mmol),  $\text{SrCl}_2$  (100 mg, 0.375 mmol),  $\text{Mg}(\text{CH}_3\text{COO})_2$  (50 mg, 0.234 mmol), and cyclohexane (0.5 mL) were added, and the resultant pale orange/pink mixture was stirred vigorously for 20 min. Potassium carbonate was then added until the solution became pink (approximately pH 5), at which time it was filtered and layered with 2-propanol. After 6 days, pink prism crystals of  $\text{Sr}_4\text{Co}_4\text{I}_2 \cdot \text{C}_6\text{H}_{12} \cdot x\text{H}_2\text{O}$  formed (42 mg, 0.011 mmol, 55% yield). Anal. Calcd for  $\text{C}_{112}\text{H}_{104}\text{Co}_4\text{Sr}_4\text{N}_8\text{O}_{48} \cdot \text{C}_6\text{H}_{12} \cdot 39\text{H}_2\text{O}$ : C, 38.27; H, 5.28; N, 3.03. Found C, 38.31; H, 4.35; N, 3.01.

**X-ray Crystallography for Compounds  $\text{Mg}_2\text{K}_4\text{Co}_4\text{I}_2$  and  $\text{Sr}_4\text{Co}_4\text{I}_2$ .** Crystallographic and structural refinement data are listed in Table 2. The data for  $\text{Mg}_2\text{K}_4\text{Co}_4\text{I}_2$  were collected on a Bruker SMART CCD diffractometer at  $-100$  °C while the data for  $\text{Sr}_4\text{Co}_4\text{I}_2$  were collected using a Bruker P4 diffractometer at ambient temperature. Both diffractometers used graphite-monochromated Mo K $\alpha$  radiation ( $\lambda = 0.71073$  Å). Lattice parameters for the compounds were calculated using a least-squares procedure involving carefully centered reflections. The solution and refinement of each structure was carried out using the SHELXTL PC program packages.<sup>11</sup> Partial structures were obtained using direct methods,

- (11) Sheldrick, G. M. *SHELXTL PC*, version 5.03; Bruker Analytical X-ray Systems: Madison, WI, 1994.

### Cation Control of Pore and Channel Size

and the structures were completed using Fourier methods. The non-hydrogen atoms were refined anisotropically, except for oxygens of partial occupancy. The positions of the hydrogen atoms bound to carbon atoms in the structure were calculated, and the hydrogen atoms were allowed to ride on their neighboring carbon atoms during the refinement. Complex  $\text{Sr}_4\text{Co}_4\mathbf{1}_2$  had disordered strontium and cobalt (4:1 ratio) as countercations. The cobalt counterions were slightly displaced from the strontium, and the countercations were coordinated to carboxylate oxygens from the resorcinarene as well as to water molecules. In the structures of the complexes there were loosely held solvent water molecules outside of the cavity and disordered molecules within the cavity. These disordered molecules were given partial occupancy and resulted in the  $R$  values for  $\text{Mg}_2\text{K}_4\text{Co}_4\mathbf{1}$  being greater than desired. Due to the loss of water by both compounds, crystals of  $\text{Mg}_2\text{K}_4\text{Co}_4\mathbf{1}$  were rapidly frozen and crystals of  $\text{Sr}_4\text{Co}_4\mathbf{1}_2$  were immersed in mother liquor and sealed in a capillary tube for data collection.

**Thermogravimetric Analysis.** Samples 1–5 mg in size were used for analysis. The samples were heated to 180 °C and cooled to the desired temperature (25–95 °C) under a nitrogen purge. Once

at the desired temperature, water vapor was passed over the samples and their weight gain was recorded, after which the samples were heated and dried again. The same sample was used for a given adsorption study. Equilibrium constants,  $K_{\text{ad}}$ , were calculated by using  $K_{\text{ad}} = [\text{H}_2\text{O on surface}]/[\text{surface without H}_2\text{O}](\text{H}_2\text{O vapor pressure})$ . Generating a van't Hoff plot by plotting the  $\ln K_{\text{ad}}$  versus inverse temperature ( $\text{K}^{-1}$ ) gives a slope that is proportional to the heat of adsorption,  $\Delta H$ . A straight line was drawn to find the slope, even though we realized the curves were not exactly linear and that there might be more than one site of water binding. Thus, the heats of adsorption are an average value for the water in the materials.

**Acknowledgment.** We thank Brigham Young University for its financial support.

**Supporting Information Available:** X-ray crystallographic files for  $\text{Mg}_2\text{K}_4\text{Co}_4\mathbf{1}_2$  and  $\text{Sr}_4\text{Co}_4\mathbf{1}_2$  (CIF). This material is available free of charge via the Internet at <http://pubs.acs.org>.

IC011135O